One-hole dynamics in the anisotropic three-dimensional t-J model

1994 J. Phys.: Condens. Matter 6 4129

(http://iopscience.iop.org/0953-8984/6/22/012)

J. Phys.: Condens. Matter 6 (1994) 4129–4136. Printed in the UK

One-hole dynamics in the anisotropic three-dimensional t–J model

Weijie Zhang and Juelian Shen

China Centre of Advanced Science and Technology (World Laboratory), PO Box 8730, Beijing 100080, People's Republic of China, and Institute of Physics, PO Box 603, Beijing 100080, People's Republic of China

Received 28 September 1993, in final form 7 December 1993

Abstract. We have studied one-hole dynamics in a quantum antiferromagnet by use of the anisotropic three-dimensional t–J model in the simple cubic lattice within the self-consistent Born approximation. The hole spectral function, the density of states, the quasiparticle dispersion relationship, the effective mass, the quasiparticle spectral weight, and the incoherent multiple spin-wave background are determined as functions of the Heisenberg exchange and hopping amplitude in the thermodynamic limit.

Hole motion in the two-dimensional (2D) t–J model has been intensively studied during recent years. This is because this model is believed [1] to contain the low-energy physics of the high-T_c cuprate materials. As a first, but important step, one hole in the spin background has been first considered by Schmitt-Rink and co-workers [2] as well as Kane and co-worker [3]. Further investigations and simulations on small 2D clusters have been performed to extract information in the thermodynamic limits (see, for example [4–7]). It is now clear that the spectral function of one hole in the 2D antiferromagnet consists of a quasiparticle peak followed by a broad incoherent background which reflects real multiple spin-wave processes accompanying hole motion. The lowest-energy quasiparticle state has momentum $k = (\pi/2, \pi/2)$.

In this paper, we present our study of one-hole motion in the quantum antiferromagnet by use of the anisotropic three-dimensional (A3D) t–J model in the simple cubic lattice within the self-consistent Born approximation. The reason that motivates us is that experiments [8] indicate that interactions between the CuO_2 planes are not trivial and may play an important role in determining the superconducting transition temperature [9]. Furthermore, the results previously obtained [2–7] in the t–J model depend on the dimensionality. In the A3D t–J model, we consider the hopping amplitude t and the Heisenberg exchange J in the xy plane. They are $t_\perp$ and $J_\perp$ in the z direction with values from zero to t and from zero to J, respectively. Calculations are performed by use of an iterative technique and the special integration method in the Brillouin zone [10].

Let us begin with the A3D t–J model in the simple cubic lattice,

$$H = -\sum_{\langle i,j\rangle\sigma} t_{ij} c_{i\sigma}^{\dagger} c_{j\sigma} + \sum_{\langle i,j\rangle} J_{ij} S_i \cdot S_j \tag{1}$$

where $c_{i\sigma}$ is the projected electron operator with spin σ at site i, taking into account that double occupancy of sites is not allowed, and S_i is the electron spin operator. Here $\langle i, j\rangle$

0953-8984/94/224129+08$19.50

indicates sum over pairs of nearest neighbours, and $t_{ij} = t$, $J_{ij} = J$ for the nearest-neighbouring i, j in the xy plane and $t_{ij} = t_\perp$, $J_{ij} = J_\perp$ for the nearest-neighbouring i, j in the z direction. Both $g \equiv J_\perp/J$ and $\delta \equiv t_\perp/t$ are between zero and unity with $\delta = g = 0$ corresponding to the 2D t–J model.

Following Kane and co-workers [3], we express the projected electron operators in the 'slave fermion' representation, $c^\dagger_{i\sigma} \to f_i b^\dagger_{i\sigma}$, where the Schwinger boson operator $b_{i\sigma}$ keeps track of the spins, and the slave fermion f_i annihilates a hole state at site i. The operators $b_{i\sigma}$ and f_i are subject to the constraint that $f^\dagger_i f_i + \Sigma_\sigma b^\dagger_{i\sigma} b_{i\sigma} = 1$ on each site. Through the same procedure as used in [3], the Néel-ordered state can be considered as a condensate of $b_{1i\downarrow}(b_{2j\uparrow})$ Bose fields in a 1(2) sublattice and uncondensed bosons $b_{1i\uparrow}(b_{2j\downarrow})$ turn into spin-wave excitation operators in the Néel background. Replacing $b_{1i\downarrow}$ and $b_{2j\uparrow}$ by $\sqrt{2S}$ and absorbing $\sqrt{2S}$ into t_{ij}, we can obtain the effective Hamiltonian [2, 3],

$$H = H_t + H_J \tag{2}$$

$$H_t = -\sum_{\langle i,j\rangle} t_{ij} f_i f^\dagger_j (b^\dagger_{1i\uparrow} + b_{2j\downarrow}) + \text{HC} \tag{3}$$

$$H_J = \tfrac{1}{2}\sum_{\langle i,j\rangle} J_{ij}(b^\dagger_{1i\uparrow} b_{1i\uparrow} + b^\dagger_{2j\downarrow} b_{2j\downarrow} + b^\dagger_{1i\uparrow} b^\dagger_{2j\downarrow} + b_{1i\uparrow} b_{2j\downarrow}). \tag{4}$$

The H_J can be diagonalized by Fourier and Bogliubov transformation,

$$b_k = \frac{1}{\sqrt{N}}\left(\sum_{i\in 1} b_{1i\uparrow} e^{ik\cdot r_i} + \sum_{j\in 2} b_{2j\downarrow} e^{ik\cdot r_j}\right) \tag{5}$$

$$\begin{pmatrix} \beta_k \\ \beta^\dagger_{-k} \end{pmatrix} = \begin{pmatrix} u_k & -v_k \\ -v_k & u_k \end{pmatrix} \qquad \begin{pmatrix} b_k \\ b^\dagger_{-k} \end{pmatrix} \tag{6}$$

where $u_k = \{[(1-\gamma_k^2)^{-1/2} + 1]/2\}^{1/2}$ and $v_k = -\text{sgn}(\gamma_k)\{[(1-\gamma_k^2)^{-1/2} - 1]/2\}^{1/2}$ with $\gamma_k = 2[\cos k_x + \cos k_y + g\cos k_z]/z$ and $z = 4 + 2g$. The spin wave dispersion is $\omega_k = zJ[1-\gamma_k^2]^{1/2}$.

The Hamiltonian then reads

$$H = -\frac{z_1 t}{N^{1/2}} \sum_{k,q} f_k f^\dagger_{k-q}[P(k,q)\beta_{-q} + Q(k,q)\beta^\dagger_q] + \sum_k \omega_k \beta^\dagger_k \beta_k \tag{7}$$

where $P(k,q) = (\eta_{k-q} v_q + \eta_k u_q)$ and $Q(k,q) = (\eta_{k-q} u_q + \eta_k v_q)$ with $\eta_k = 2[\cos k_x + \cos k_y + \delta \cos k_z]/z_1$ and $z_1 = 4 + 2\delta$. The first term in equation (7) indicates the coupling term between hole and spin waves and the second term is the spin background under the linear spin-wave approximation [2, 3, 6].

The one-hole retarded Green's function is defined as

$$G(k,\omega) = \langle 00| f_k[\omega - H + i0^+]^{-1} f^\dagger_k|00\rangle \tag{8}$$

where $|00\rangle$ represents the vacuum state of hole and spin waves. One can easily obtain the equation [11]

$$\begin{aligned} G(k,\omega) = G^0(k,\omega) &+ \frac{z_1^2 t^2}{N} G^0(k,\omega) \sum_{p,q} P(k-q,-q) Q(p,q) \\ &\times \langle 00| f_{k-q}[\omega - H - \omega_q]^{-1} f^\dagger_{p-q} f_p[\omega - H]^{-1} f^\dagger_k|00\rangle \end{aligned} \tag{9}$$

where $G^0(k,\omega) = [\omega + \mathrm{i}0^+]^{-1}$. In the self-consistent Born approximation, we obtain the two integral equations

$$G(k,\omega) = G^0(k,\omega) + G^0(k,\omega)\Sigma(k,\omega)G(k,\omega) \tag{10}$$

$$\Sigma(k,\omega) = \frac{z_1^2 t^2}{N}\sum_q Q^2(k,q)G(k-q,\omega-\omega_q). \tag{11}$$

As usual the hole spectral function is

$$A(k,\omega) = -\,\mathrm{Im}\,G(k,\omega+\mathrm{i}0^+). \tag{12}$$

The self-consistent equations (10) and (11) are solved numerically using the iteration technique. In this paper, we always fix $t = 1$ eV as the energy unit. To make the iteration procedure stable, an artificial broadening parameter $\epsilon \ll t$ is introduced [4–7]. The iteration is carried out until the needed convergence is achieved. We employ the integration method developed by Chadi and Cohen [10]. The method is to determine a set of special wave-vector points in the Brillouin zone which is the most efficient for purposes of accurately calculation the averages of a periodic function over the Brillouin zone.

In general, the integrand in (11) does not have the symmetries of $(k_x,k_y,k_z) \leftrightarrow (k_z,k_y,k_x)$ and $(k_x,k_y,k_z) \leftrightarrow (k_x,k_z,k_y)$. A set of 40 special points [10] in the irreducible 3D Brillouin zone ($k_x \geqslant k_y \geqslant 0, k_z \geqslant 0$) are used. Due to the symmetries of the Green function, the calculation can be limited to the irreducible part of the Brillouin zone [6]. This irreducible part can be extended to the rest of the zone by use of a symmetry operation.

First we calculate the hole spectral function and other properties in the 2D case, i.e., $\delta = g = 0$. We have reproduced all the results of Marsiglio and co-workers [6]. For example, the solid line in figure 1(a) is the hole spectral function at $k = (\pi/2, \pi/2)$ with $J = 0.1$. This is the same as figure 5(a) in [6].

The density of states $D(\omega)$ is defined as

$$D(\omega) = (\pi N)^{-1}\sum_k A(k,\omega). \tag{13}$$

The solid line in figure 1(b) shows $D(\omega)$ in the 2D case with $J = 0.1$.

The quasiparticle energy ϵ_k is obtained by solving the self-consistent equation

$$\epsilon_k = \mathrm{Re}\,\Sigma(k,\epsilon_k) \tag{14}$$

while $\mathrm{Im}\,\Sigma(k,\epsilon_k)$ must vanish [2–7]. The quasiparticle spectral weight z_k is

$$z_k = \left[1 - \frac{\partial\,\mathrm{Re}\,\Sigma(k,\omega)}{\partial\omega}\right]^{-1}\Bigg|_{\omega=\epsilon_k}. \tag{15}$$

Since a finite ϵ is needed in the calculation, the calculated valued of ϵ_k, $\mathrm{Im}\,\Sigma(k,\epsilon_k)$ and z_k are influenced by the choice of ϵ. In the 2D case for $J = 0.1$ with $\epsilon = 0.01$, 0.005, and 0.0025, the calculated values of ϵ_k for $k = (\pi/2, \pi/2)$ are -2.5287, -2.5291, and -2.5293, for respective values of ϵ. The values of z_k are 23.19, 23.23, and 23.25%, respectively. The quasiparticle dispersion relationship is also calculated. The values of ϵ_k for $k = (\pi, 0)$ and $k = (0, 0)$ are -2.4404 and -2.0862 respectively. Our results are almost the same as the results of the thermodynamic limits of Marsiglio and co-workers [6]. These results are

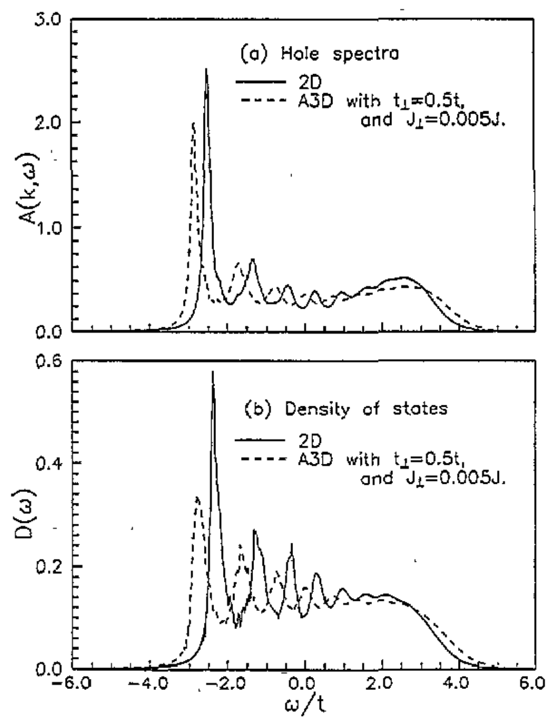

Figure 1. (a) Hole spectral function for the 2D t–J model with $J = 0.1t$ at $k = (\pi/2, \pi/2)$ (the solid line) and for the A3D case at $k = (\pi/2, \pi/2, 0)$ with $J = 0.1t$, $\delta = 0.5$, and $g = 0.005$ (the dashed line). (b) The density of states for the 2D case with $J = 01t$ (the solid line) and for the A3D case with $J = 0.1t$, $\delta = 0.5$, and $g = 0.005$ (the dashed line).

also in general agreement with exact 4×4 cluster results of Dagotto and co-workers [5] and recent results of Barnes and co-workers [7].

Next we treat the A3D cases. We find that the quasiparticle picture still holds in the whole range of $\delta(\delta = t_\perp/t)$ and $g(g = J_\perp/J)$ (both δ and g range from zero to unity). At each momentum, the hole spectral function consists of a quasiparticle peak and broad incoherent background due to the multiple spin-wave excitation. For example, the dashed line in figure 1(a) shows the hole spectral function at $k = (\pi/2, \pi/2, 0)$ for $J = 0.1$, $g = 0.005$, and $\delta = 0.5$. The corresponding density of states is shown in figure 1(b) (the dashed line). The quasi-two-dimensional (Q2D) case, where $t_\perp$ and $J_\perp$ are small, is experimentally the most interesting, since the high-T_c materials are the layered copper oxide compounds. We find that for $g < 0.03$, the spectral weight and the peak height of the quasiparticle are smaller than those in the exact 2D case. Correspondingly, the spectral weight of the incoherent multiple spin-wave background and its energy extension range become larger than those in the exact 2D case.

We have calculated the quasiparticle dispersion along the symmetry direction for $J = 0.1$ with various sets of δ and g. The momenta corresponding to the quasiparticle states determine the excitation properties of the quasiparticles and the lowest-energy quasiparticle state determines the hole ground state. In the exact 2D cases, the lowest-energy quasiparticle state locates at $k = (\pi/2, \pi/2)$ [2–7]. In A3D cases, our calculations show that the lowest-energy quasiparticle state has momentum either at $k = (\pi/2, \pi/2, 0)$, or $k = (\pi/2, \pi/2, \pi/2)$, depending on the parameters of the models. For illustration,

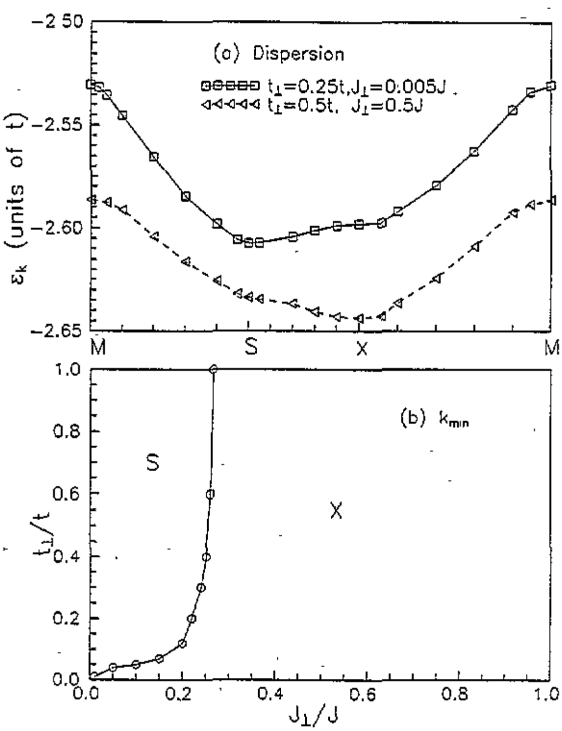

Figure 2. (a) Quasiparticle dispersion along the symmetry directions in the A3D cases for $J = 0.1t$ with $\delta = 0.25$ and $g = 0.005$ (the solid line) and with $\delta = g = 0.5$ (the dashed line). Here M, S and X represent the momentum at $k = (\pi, 0, 0)$, $k = (\pi/2, \pi/2, 0)$, and $k = (\pi/2, \pi/2, \pi/2)$, respectively. (b) The momentum of the lowest-energy quasiparticle state as a function of the set of δ and g. In the wedge marked S, it has momentum $k = (\pi/2, \pi/2, 0)$. In the wedge marked X, it has $k = (\pi/2, \pi/2, \pi/2)$. In the range of $\delta \leqslant 0.01$ and $g \leqslant 0.01$, the quasiparticle states at these two momenta are degenerate.

figure 2(a) shows the results for $\delta = 0.25$ with $g = 0.005$ (the solid line) and for $\delta = 0.5$ with $g = 0.5$ (the dashed line). The lowest-energy quasiparticle state, $\epsilon_{\min}$, has momentum $k = (\pi/2, \pi/2, \pi/2)$ or $k = (\pi/2, \pi/2, 0)$, depending on the values of δ and g. In figure 2(b), a critical line exists in the δ-g diagram on which the quasiparticle states are degenerate at these two momenta. Above the critical line, $\epsilon_{\min}$ has momentum $k = (\pi/2, \pi/2, 0)$ while it has momentum $k = (\pi/2, \pi/2, \pi/2)$ below this line. For $g \geqslant 0.26$, $\epsilon_{\min}$ has momentum $k = (\pi/2, \pi/2, \pi/2)$ in the whole range of δ from zero to unity. For $\delta \leqslant 0.01$ and $g \leqslant 0.01$, they are degenerate. In the low-density hole doping limits of experimental interest, $g \simeq 0.005$ and $t_\perp \simeq 20$ K, hence in this case they are degenerate.

The effective mass m^* can be obtained from ϵ_k,

$$\left[\frac{1}{m^*}\right]_{ij} = \frac{\partial^2 \epsilon_k}{\partial k_i \partial k_j}. \tag{16}$$

Figure 3 shows that the inverse effective mass at the bottom of the band along the z-direction, $1/m_z^*$, as a function of g for the cases with $J = 0.1t$ and several values of $t_\perp$. In general, for the cases with g fixed, the larger $t_\perp$ is, the larger $1/m_z^*$ is. For the cases with the set of δ and g on the critical line in figure 2(b), m_z^* is infinity. Fixing $t_\perp$, as g

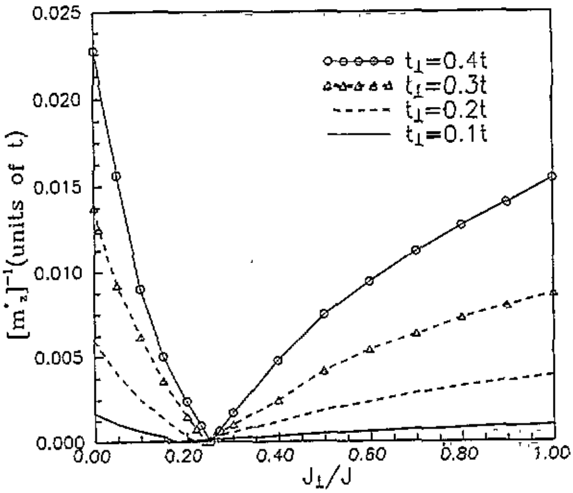

Figure 3. The inverse of the quasiparticle effective mass at the bottom of the band along the z-direction as a function of $J_\perp/J$ in the cases with $J = 0.1t$ and various values of $t_\perp$.

increases, the value of $1/m_z^*$ first decreases when $\epsilon_{\rm min}$ has momentum $k = (\pi/2, \pi/2, 0)$ and then increases when $\epsilon_{\rm min}$ has $k = (\pi/2, \pi/2, \pi/2)$.

In the exact 2D cases, a number of papers has been devoted to studying the dependence of the quasiparticle properties on the values of t and J. However, those results are limited to 2D. It is important to study the influence of the anisotropic structure of A3D cases on the quasiparticle properties, that is, to study the dependence of the quasiparticle properties on the values of δ and g with fixed in-plane values of t and J. This is because even in the zero-temperature limit, the A3D cases are closer to the real physical object of the layered copper oxide compounds than the exact 2D cases. Let J be fixed to be 0.1. We find that fixing g (in the whole range from zero to unity), with increasing δ, the spectral weight z_k and the peak height of the quasiparticle decrease. On the other hand, fixing δ (in the whole range from zero to unity), with increasing g, the spectral weight z_k and the peak height increase. Figure 4 shows z_k and $-\operatorname{Im}\Sigma(k, \epsilon_k)$ of the quasiparticle at $k = (\pi/2, \pi/2, 0)$ as functions of δ for $g = 0.05$ (figure 4(a)) and as functions of g for $\delta = 0.2$ (figure 4(b)) (the value of ϵ is 0.005 in both cases). In the cases shown in figure 4(a), one can see that as δ goes from zero to unity, the spectral weight z_k decreases from 24.26 to 14.75% and the peak height, which is $[-\operatorname{Im}\Sigma(k, \epsilon_k)]^{-1}$, decreases from 48.92 to 29.76 (in units of t^{-1}). In the case shown in figure 4(b), as g goes from zero to unity, the spectral weight z_k increases from 22.93 to 28.75% and the peak height increases from 46.21 to 57.92. The reason that a profound quasiparticle peak exists in the whole range of δ and g is that there is a small density of states of low-lying spin excitations. The broad incoherent structure reflects the real multiple spin-wave processes accompanying hole motion. As discussed in [6], the quantum antiferromagnet treats the spin ground state as a linear combination of the Néel state and states with multiple zero-point spin deviations. When the hole hops, it also creates spin deviations. Hence, the spin configuration, after one hole hop, has a finite overlap with the configuration prior to the hop. This leads to Bloch-like propagation. The quasiparticle spectral weight is proportional to this overlap. Thus consider the A3D cases with J held constant. Fixing $J_\perp$ and increasing $t_\perp$, the overlap between the spin configuration after and prior to a hop decreases. Fixing $t_\perp$ and increasing $J_\perp$, the overlap increases. In the Q2D case with small $t_\perp$ and $J_\perp$, the overlap is smaller than that in the 2D case.

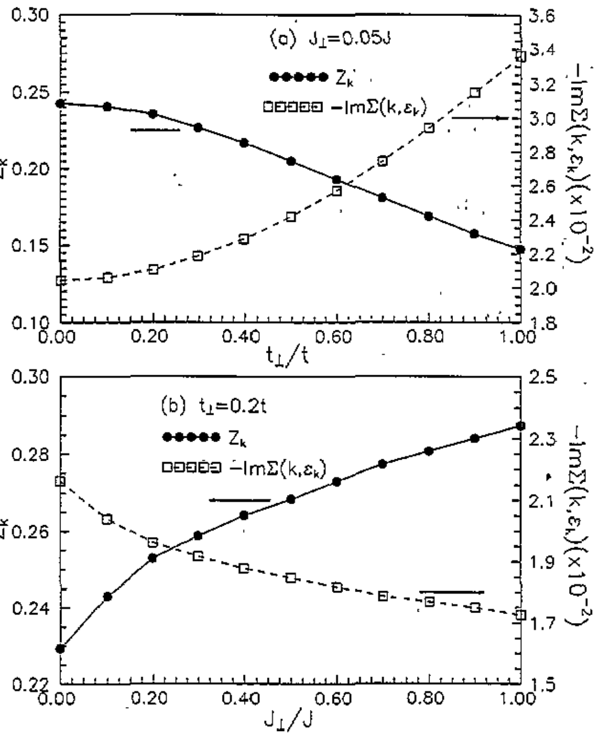

Figure 4. For the quasiparticle at $k = (\pi/2, \pi/2, 0)$, the spectral weight z_k and $-\operatorname{Im}\Sigma(k, \epsilon_k)$ (a) as functions of δ with $g = 0.05$ and (b) as functions of g with $\delta = 0.2$. In each figure, the solid line represents z_k (the left-hand scale) and the dashed line represents $-\operatorname{Im}\Sigma(k, \epsilon_k)$ (the right-hand scale).

In conclusion, we have studied one-hole dynamics in the A3D t–J model within the self-consistent Born approximation. Hole spectra, the density of states, the quasiparticle spectral weight, the dispersion relationship, the effective mass, and the incoherent multiple spin-wave background are determined as functions of $t_\perp$ and $J_\perp$ by use of an iterative technique. The lowest-energy quasiparticle state has momentum either at $k = (\pi/2, \pi/2, 0)$, or $k = (\pi/2, \pi/2, \pi/2)$, depending on the parameters of the models. The behaviour of the effective mass along the z direction is also different depending on where $\epsilon_{\min}$ locates. Holding J constant, fixing $J_\perp(t_\perp)$ and increasing $t_\perp(J_\perp)$, the spectral weight and the peak height of the quasiparticle decrease (increase). It is important to note that in the Q2D case, the spectral weight and the peak height of the quasiparticle are smaller than those in the exact 2D case. Correspondingly, the spectral weight of the incoherent multiple spin-wave background and its energy extension range become larger than those in the exact 2D case.

Acknowledgments

This work is supported by the National Centre for Research and Development on Superconductivity of China and by the grant LWTZ-1298 of the Chinese Academy of Sciences.

References

[1] Anderson P W 1987 *Science* **235** 1196
[2] Schmitt-Rink S, Varma C M and Ruckenstein A E 1988 *Phys. Rev. Lett.* **60** 2793
[3] Kane C L, Lee P A and Read N 1989 *Phys. Rev.* B **39** 6880
[4] Trugman S A 1988 *Phys. Rev.* B 37 1597
[5] Dagotto E, Joynt R, Moreo A, Bacci S and Gagliano E 1990 *Phys. Rev.* B **41** 9049
[6] Marsiglio F, Ruckenstein A E, Schmitt-Rink S and Varma C M 1991 *Phys. Rev.* B **43** 10 882
[7] Barnes T, Jacobs A E, Kovarik M D and Macready W G 1992 *Phys. Rev.* B **45** 256
[8] See for example, Salamon M B 1990 *Physical Properties of High Temperature Superconductors* ed D M Ginsberg (Singapore: World Scientific) p 39
[9] Anderson P W 1992 *Science* **256** 1526
[10] Chadi D J and Cohen M L 1973 *Phys. Rev.* B 7 692
[11] Messiah A 1962 *Quantum Mechanics* (Amsterdam: North-Holland)